nature geoscience

SUPPLEMENTARY INFORMATION

DOI: 10.1038/NGEO1568

Sensitivity of tropical precipitation extremes to climate change

Paul A. O'Gorman

1 Climate-model simulations

The 18 CMIP3 models used are BCCR-BCM2.0, CGCM3.1 T47, CGCM3.1 T63, CNRM-CM3, CSIRO-Mk3.0, CSIRO-Mk3.5, GFDL-CM2.0, GFDL-CM2.1, FGOALS-g1.0, ECHAM4/INGV, ECHAM5/MPI, INM-CM3.0, IPSL-CM4, MIROC3.2-med, MIROC3.2-hi, MRI-CGCM2.32, NCAR-PCM1, and NCAR-CCSM3.0. The time periods used are 1981-2000 (20C3M) and 2081-2100 (SRES A1B), except for BCCR-BCM2.0 (1981-1998, 2081-2098), CNRM-CM3 (1981-1999, 2081-2099), FGOALS-g1.0 (1981-1999, 2081-2099), MIROC3.2-hi (1981-1999, 2081-2099), NCAR-PCM1 (1980-1999, 2080-2098), and NCAR-CCSM3.0 (1980-1999, 2080-2099). Models not included in the analysis were primarily excluded because of lack of availability of the necessary data or because of corrupt data. The GISS-AOM model was excluded because it has extremely weak ENSO temperature variability[S1] (it also gives a negative sensitivity of precipitation extremes for variability). Inspection of Fig. 2 suggests that the two GFDL models may be influential in the regression of sensitivities; omitting the GFDL models from the analysis changes the inferred sensitivity for climate change of the 99.9th percentile of precipitation from $10\%\mathrm{K}^{-1}$ to $8\%\mathrm{K}^{-1}$. (The inferred sensitivity using the CMIP5 ensemble remains at $11\%\mathrm{K}^{-1}$ if the GFDL models are omitted.)

The CMIP3 models with relatively-good simulations of ENSO (the "good-ENSO" models) are taken to be ECHAM5/MPI, GFDL-CM2.0, GFDL-CM2.1, IPSL-CM4, and MRI-CGCM2.32. This subset of models follows the selection in a previous study[S1], with the exception of the UKMO-HadCM3 model for which the necessary daily data were not available.

The 15 CMIP5 models used are ACCESS1.0, BNU-ESM, CCSM4, CSIRO-Mk3.6.0, GFDL-ESM2G, GFDL-ESM2M, GFDL-CM3, HadGEM2-CC, HadGEM2-ES, IPSL-CM5A-MR, IPSL-CM5B-LR, MIROC-ESM-CHEM, MIROC5, MRI-CGCM3, and NorESM1-M. The time periods used are 1981-2000 (historical) and 2081-2100 (RCP 8.5), except for ACCESS1.0 (1980-1999, 2081-2100), GFDL-CM3 (1980-1999, 2081-2100), HadGEM2-CC (1981-2000, 2081-2099), HadGEM2-ES (1981-2000, 2081-2099), IPSL-CM5A-MR (1980-1999, 2081-2100), MIROC5 (1980-1999, 2080-2099), MRI-CGCM3 (1980-1999, 2081-2100), and NorESM1-M (1980-1999, 2081-2100).

2 Observational precipitation datasets

The default precipitation observations used are based on passive-microwave retrievals and are taken from the SSM/I (V6) dataset[S2] of Remote Sensing Systems (RSS) for the period 1991-2008 using the satellites F10 (1991-1995) and F13 (1996-2008). The time series could have been extended three years further back in time by also using F08, but using only two satellites helps to minimize uncertainties related to intercalibration. Results for four other observational datasets are presented in Fig. S6 and Table S4, and the time periods used are specified in Table S4. SSM/I GPROF refers to version 10 of the Goddard Profiling Algorithm[S3] using the same satellites and time periods as for

the default SSM/I dataset. The Tropical Rainfall Measuring Mission (TRMM) Microwave Imager (TMI) dataset used is also based on the GPROF version 10 algorithm. The 1-degree daily merged product V1.1 from the Global Precipitation Climatology Project (GPCP 1DD) includes inputs from infrared, passive-microwave, and gauge measurements[S4]. The TRMM 3B42 V7 merged daily dataset includes inputs from infrared, passive and active microwave, and gauge measurements[S5]. Taken together, the observational datasets for precipitation include different satellites, types of sensors, and retrieval algorithms, although they are not independent.

TRMM 3B42 has somewhat different variability from the other datasets in the case of mean precipitation, but it gives similar results to the other datasets in the case of precipitation extremes (Fig. S6). An earlier version (V6) was found to be inconsistent with the other datasets as regards interannual variability of both mean and extreme precipitation, a discrepancy that is noted in previous papers[S5,S6].

Daily precipitation is accumulated in models but must be combined from estimates at discrete times during the day in satellite observations. This may be expected to affect the absolute daily precipitation rates, but not necessarily their fractional changes. Some confidence that this issue does not strongly impact the final results comes from the similarity of inferred sensitivities (Table S4) from SSM/I (at most one ascending and one descending pass per day at each location), TMI (a similar number of passes but with different orbital characteristics from SSM/I), and the merged datasets GPCP 1DD and TRMM 3B42.

3 Dependence on tropical cyclones and choice of domain

The high precipitation percentiles considered in this study include contributions from a range of different types of tropical systems, including tropical cyclones. To assess the influence of tropical cyclones on the results, the analysis was repeated over the latitude band 5S to 5N in which there is little tropical-cyclone activity. Although the relationship between sensitivities for variability and climate change is not as strong for this narrower latitude band, similar results are obtained for the inferred sensitivity for climate change. For the 99.9th percentile of precipitation, the inferred sensitivity is $11\%\mathrm{K}^{-1}$ when 5S to 5N is used compared with $10\%\mathrm{K}^{-1}$ when 30S to 30N is used.

More generally, the calculated sensitivity for variability depends on the domain chosen (e.g., which parts of the Pacific are included or how much land is included) because of the spatially-heterogeneous response of precipitation to ENSO. But this does not imply that the inferred sensitivity for climate change depends strongly on the choice of domain because both modeled and observed sensitivities for variability are affected by the choice of domain. For example, for the 99.9th percentile of precipitation and the SSM/I GPROF precipitation dataset, the sensitivity for variability is $33\%\mathrm{K}^{-1}$ over ocean and $21\%\mathrm{K}^{-1}$ over the whole tropics, while the resulting inferred sensitivities for climate change are $13\%\mathrm{K}^{-1}$ in both cases. However, it is important that land is masked out in a consistent way in both the models and observations. Results based on variability over land alone are not reported because this gives a sensitivity for variability that is not strongly related to the response to climate change.

4 Dependence on method of calculation of precipitation extremes

The sensitivities of tropical precipitation extremes for climate change calculated here are similar but not exactly the same as those in a previous study[S7], the results of which are used for comparison. In particular, the multimodel-median sensitivity in the tropics for the 99.9th percentile of precipitation is similar at $6\%\mathrm{K}^{-1}$ in this study and $5\%\mathrm{K}^{-1}$ in ref. S7, but the intermodel scatter is smaller in this study. The differences arise because of slightly different sets of climate models used and different methods of aggregation of precipitation rates, and because the precipitation rates used here are interpolated to a common grid prior to calculation of percentiles. In ref. S7, precipitation rates are aggregated at each latitude over the entire time period prior to calculating percentiles, and percentage changes in the precipitation percentiles are then averaged in latitude over the tropics or extratropics. The inferred sensitivity for climate change of the 99.9th percentile of tropical precipitation increases by only $0.1\%\mathrm{K}^{-1}$ when the analysis presented here is repeated using the aggregation method of ref. S7 for climate-change sensitivities. If the precipitation percentiles are also calculated on the native model grids when calculating climate-change sensitivities, the intermodel scatter increases to what was found in ref. S7 and the inferred sensitivity for climate change increases from 10 to $12\%\mathrm{K}^{-1}$, but with a wider 90% confidence interval of 6 to $17\%\mathrm{K}^{-1}$. The thermodynamic rates and simulated extratropical sensitivities are more robust than the simulated tropical sensitivities so that it is reasonable to use the values calculated in ref. S7 as a point of comparison for the inferred sensitivities calculated here.

Supplementary references

S1. Guilyardi, E. *et al.* Understanding El Niño in ocean–atmosphere general circulation models. *Bull. Amer. Meteor. Soc* **90**, 325–340 (2009).

S2. Hilburn, K. A. & Wentz, F. J. Intercalibrated passive microwave rain products from the unified microwave ocean retrieval algorithm (UMORA). *J. Appl. Meteorol.* **47**, 778–794 (2008).

S3. Kummerow, C. *et al.* The evolution of the Goddard Profiling Algorithm (GPROF) for rainfall estimation from passive microwave sensors. *J. Appl. Meteorol.* **40**, 1801–1820 (2001).

S4. Huffman, G. J. *et al.* Global precipitation at one-degree daily resolution from multisatellite observations. *J. Hydrometeor.* **2**, 36–50 (2001).

S5. Huffman, G. J. *et al.* The TRMM multisatellite precipitation analysis (TMPA): Quasi-global, multiyear, combined-sensor precipitation estimates at fine scales. *J. Hydrometeorol.* **8**, 38–55 (2007).

S6. Liu, C. & Allan, R. P. Multisatellite observed responses of precipitation and its extremes to interannual climate variability. *J. Geophys. Res.* **117**, D03101 (2012).

S7. O'Gorman, P. A. & Schneider, T. The physical basis for increases in precipitation extremes in simulations of 21st-century climate change. *Proc. Natl. Acad. Sci.* **106**, 14773–14777 (2009).

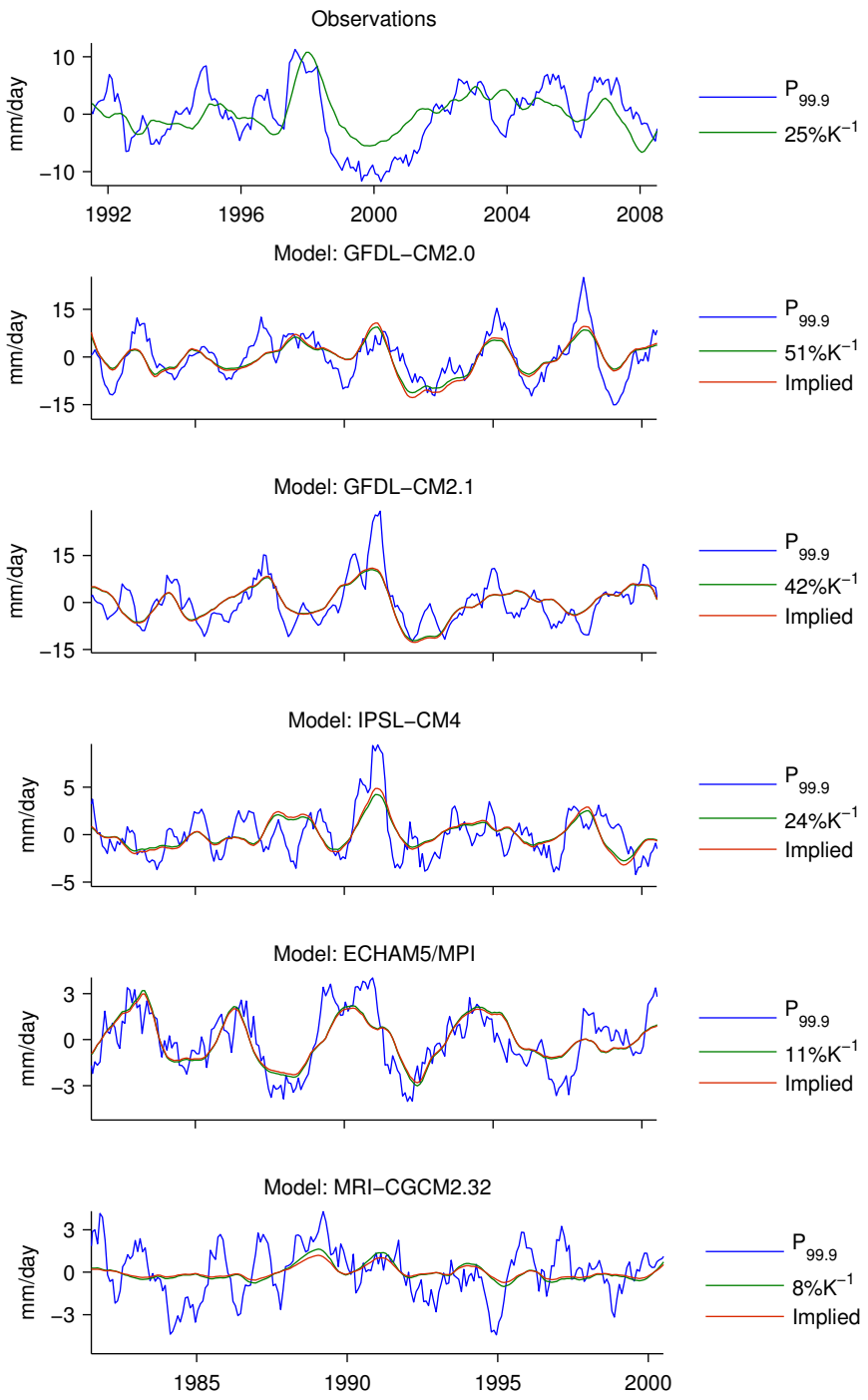

Fig. S1. As in Fig. 1 but showing time series for all of the "good-ENSO" subset of CMIP3 models.

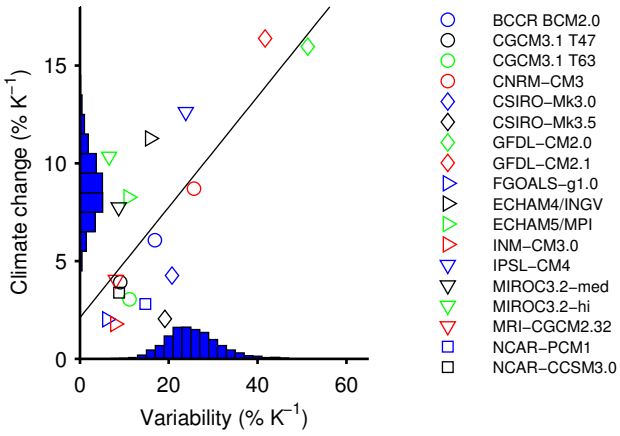

Fig. S2. As in Fig. 2 but for climate change over tropical land only. The sensitivity for climate change over land is normalized by the change in surface temperature over the whole tropics. Variability is calculated over the tropical oceans.

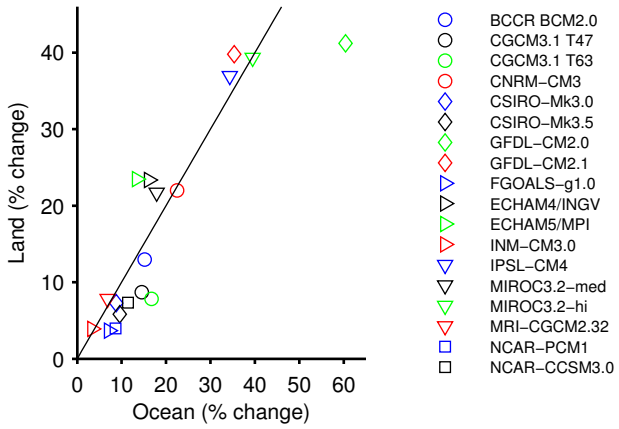

Fig. S3. Percentage changes in the 99.9th percentile of precipitation over land versus ocean in the CMIP3 simulations. The solid line corresponds to equal percentage changes over land and ocean. The correlation coefficient of percentage changes over land and ocean is 0.897. Unlike in other figures, the results shown are not normalized by changes in surface temperature.

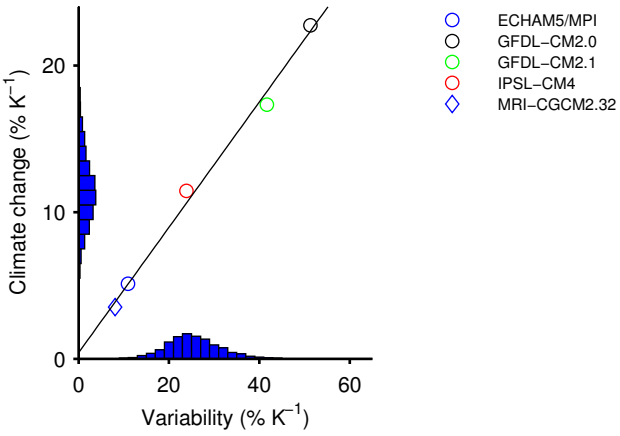

Fig. S4. As in Fig. 2 but based on the "good-ENSO" subset of CMIP3 models.

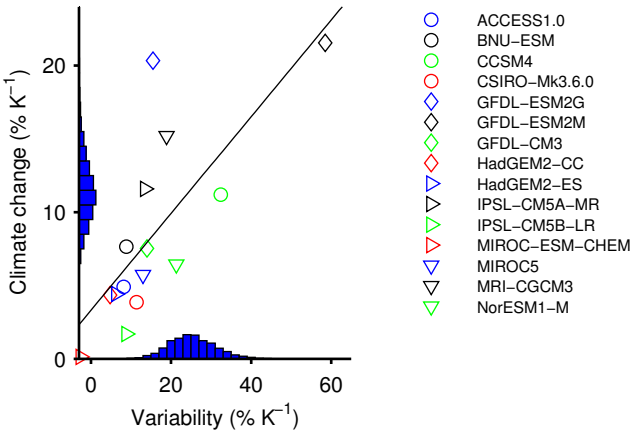

Fig. S5. As in Fig. 2 but based on the CMIP5 climate models.

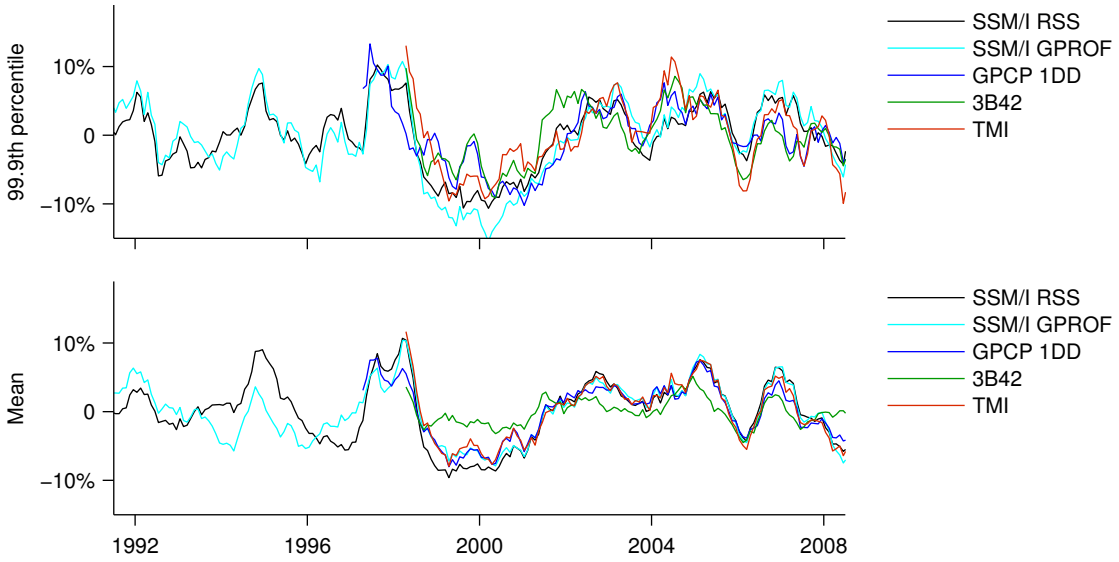

Fig. S6. Anomalies (%) in (top) the 99.9th percentile of precipitation and (bottom) mean precipitation over the tropical oceans in the default (SSM/I RSS) and four other observational datasets. Time series are filtered with a 6-month running average. Time periods differ for the different datasets and are longest for SSM/I RSS and GPROF (see Table S4).

Table S1. Inferred sensitivities for climate change with 90% confidence intervals (CIs) for different high percentiles of precipitation based on CMIP3 models and the "good-ENSO" subset of CMIP3 models. The correlation coefficient (r) and regression coefficients (a,b) for the relationship s_c=a+bs_v between the sensitivity for variability (s_v) and the sensitivity for climate change (s_c) are also given. The sensitivity for variability is over the tropical oceans, and the sensitivity for climate change is over the whole tropics.

Percentile	All Models				"Good-ENSO" models			
	Inferred s_c	r	a	b	Inferred s_c	r	a	b
	%K^{-1} (90% CI)		%K^{-1}		%K^{-1} (90% CI)		%K^{-1}	
98	3 (1, 5)	0.124	2.5	0.03	-3 (-10, 6)	-0.600	5.2	-0.26
99	6 (3, 7)	0.392	2.2	0.12	7 (-13, 15)	0.345	0.8	0.22
99.5	7 (4, 9)	0.522	2.2	0.18	10 (-8, 17)	0.753	-0.4	0.38
99.8	9 (6, 12)	0.735	2.2	0.28	10 (7, 16)	0.988	1.1	0.38
99.9	10 (6, 14)	0.866	1.4	0.37	11 (8, 17)	0.997	0.4	0.43
99.95	9 (5, 13)	0.882	1.3	0.38	9 (5, 16)	0.973	0.6	0.43

Table S2. As in Table S1 but for the response of precipitation extremes to climate change over tropical land only. To facilitate comparison with Table S1, the inferred sensitivities for climate change are normalized with respect to surface temperature change averaged over the whole tropics. Variability is calculated over the tropical oceans.

Percentile	All Models				"Good-ENSO" models			
	Inferred s_c	r	a	b	Inferred s_c	r	a	b
	%K^{-1} (90% CI)		%K^{-1}		%K^{-1} (90% CI)		%K^{-1}	
98	0 (-3, 3)	-0.398	3.6	-0.13	-3 (-14, 5)	-0.453	5.0	-0.27
99	3 (0, 6)	-0.063	3.4	-0.02	2 (-10, 7)	-0.128	3.9	-0.06
99.5	5 (2, 8)	0.199	3.3	0.08	7 (0, 13)	0.509	3.6	0.12
99.8	9 (5, 12)	0.609	2.0	0.27	10 (8, 16)	0.908	3.3	0.29
99.9	9 (6, 12)	0.735	2.1	0.28	11 (8, 15)	0.927	4.4	0.26
99.95	8 (5, 11)	0.760	2.3	0.28	10 (7, 16)	0.876	5.5	0.24

Table S3. As in Table S1 but comparing results using the CMIP3 and CMIP5 models.

Percentile	CMIP3 (All Models)				CMIP5			
	Inferred s_c	r	a	b	Inferred s_c	r	a	b
	$\%K^{-1}$ (90% CI)		$\%K^{-1}$		$\%K^{-1}$ (90% CI)		$\%K^{-1}$	
98	3 (1, 5)	0.124	2.5	0.03	5 (2, 8)	0.407	1.4	0.13
99	6 (3, 7)	0.392	2.2	0.12	8 (4, 11)	0.528	0.9	0.24
99.5	7 (4, 9)	0.522	2.2	0.18	9 (5, 14)	0.604	1.3	0.29
99.8	9 (6, 12)	0.735	2.2	0.28	10 (7, 15)	0.658	2.9	0.30
99.9	10 (6, 14)	0.866	1.4	0.37	11 (8, 16)	0.741	3.3	0.33
99.95	9 (5, 13)	0.882	1.3	0.38	10 (6, 15)	0.743	3.9	0.30

Table S4. Sensitivities of the 99.9th percentile of precipitation based on the default and alternative observational precipitation datasets and the CMIP3 models. Sensitivities for variability over the tropical oceans (s_v) and inferred sensitivities for climate change over the whole tropics (s_c) are shown.

Dataset	Time period	s_v	Inferred s_c
		$\%K^{-1}$ (90% CI)	$\%K^{-1}$ (90% CI)
SSM/I RSS (default)	1991-2008	25 (16, 36)	10 (6, 14)
SSM/I GPROF	1991-2008	33 (22, 49)	13 (7, 18)
TMI	1998-2008	33 (22, 40)	13 (7, 16)
GPCP 1DD	1997-2008	21 (14, 31)	9 (6, 12)
3B42	1998-2008	21 (12, 31)	9 (6, 12)

Table S5. As in Table S1 but comparing results using variability over ocean only or variability over the whole tropics. Climate change is over the whole tropics in both cases. The results in this table are based on the SSM/I GPROF precipitation dataset because the default precipitation dataset does not include values over land. The full set of CMIP3 models is used.

Percentile	Ocean variability				Land+ocean variability			
	Inferred s_c	r	a	b	Inferred s_c	r	a	b
	$\%K^{-1}$ (90% CI)		$\%K^{-1}$		$\%K^{-1}$ (90% CI)		$\%K^{-1}$	
98	3 (2, 4)	0.124	2.5	0.03	3 (2, 4)	0.182	2.3	0.08
99	6 (3, 7)	0.392	2.2	0.12	6 (3, 7)	0.478	1.8	0.25
99.5	8 (4, 10)	0.522	2.2	0.18	8 (4, 10)	0.555	2.0	0.30
99.8	10 (6, 14)	0.735	2.2	0.28	10 (6, 15)	0.660	2.0	0.44
99.9	13 (7, 18)	0.866	1.4	0.37	13 (7, 20)	0.793	1.6	0.56
99.95	13 (7, 19)	0.882	1.3	0.38	13 (7, 20)	0.820	1.6	0.55